HHS Public Access

Author manuscript

Mol Nutr Food Res. Author manuscript; available in PMC 2018 May 11.

Published in final edited form as:

Mol Nutr Food Res. 2017 October ; 61(10): . doi:10.1002/mnfr.201700139.

Gingerenone A, a polyphenol present in ginger, suppresses obesity and adipose tissue inflammation in high-fat diet-fed mice

Sujin Suk[1], **Gyoo Taik Kwon**[2], **Eunjung Lee**[1], **Woo Jung Jang**[1], **Hee Yang**[1], **Jong Hun Kim**[3], **N. R. Thimmegowda**[4,**], **Min-Yu Chung**[1], **Jung Yeon Kwon**[5], **Seunghee Yang**[1], **Jason K. Kim**[1,5], **Jung Han Yoon Park**[2,3,*], and **Ki Won Lee**[1,3]

[1]Major in Biomodulation, Department of Agricultural Biotechnology, Seoul National University, Seoul, Republic of Korea

[2]Department of Food Science and Nutrition, Hallym University, Chuncheon, Republic of Korea

[3]Research Institute of Agriculture and Life Sciences, Seoul National University, Seoul, Republic of Korea

[4]Chemical Biology Research Center and World Class Institute, Korea Research Institute of Bioscience and Biotechnology, Ochang, Republic of Korea

[5]Program in Molecular Medicine and Department of Medicine, Division of Endocrinology, Metabolism and Diabetes, University of Massachusetts Medical School, Worcester, MA, USA

Abstract

Scope—Ginger exerts protective effects on obesity and its complications. Our objectives here are to identify bioactive compounds that inhibit adipogenesis and lipid accumulation in vitro, elucidate the anti-obesity effect of gingerenone A (GA) in diet-induced obesity (DIO), and investigate whether GA affects adipose tissue inflammation (ATI).

Methods and results—Oil red O staining showed that GA had the most potent inhibitory effect on adipogenesis and lipid accumulation in 3T3-L1 cells among ginger components tested at a single concentration (40 μM). Consistent with in vitro data, GA attenuates DIO by reducing fat mass in mice. This was accompanied by a modulation of fatty acid metabolism via activation of AMP-activated protein kinase (AMPK) in vitro and in vivo. Additionally, GA suppressed ATI by inhibiting macrophage recruitment and downregulating pro-inflammatory cytokines.

Conclusion—These results suggest that GA may be used as a potential therapeutic candidate for the treatment of obesity and its complications by suppressing adipose expansion and inflammation.

Keywords

Adipocyte; Adipose tissue inflammation; AMP-activated protein kinase; Gingerenone A; Obesity

Correspondence: Dr. Ki Won Lee, kiwon@snu.ac.kr.
*Additional corresponding author: Jung Han Yoon Park, jyoon@hallym.ac.kr
**Present address: Government S.K.S.J.T. Institute, Bangalore, Karnataka, India-560001

Additional supporting information may be found in the online version of this article at the publisher's web-site

The authors have declared no conflict of interest.

1 Introduction

Obesity is characterized by the accumulation of excessive fat, which is associated with metabolic disorders [1]. Therefore as an important approach to prevent and/or treat obesity, it has been suggested to suppress adipose tissue expansion resulting from both increased adipocyte cell number (hyperplasia) and cell size (hypertrophy) [2]. Extra energy is stored as neutral lipids in adipocyte lipid droplets. The lipids originate from ingested triacylglycerol (TAG) in food and/or endogenous synthesis of fatty acids [3]. When the body requires energy, stored fat is degraded into free fatty acids (FFAs) and glycerol, a process referred to as lipolysis [3,4]. The FFAs are then metabolized to produce energy through mitochondrial β-oxidation [4]. Several studies have reported that enhanced energy expenditure based on β-oxidation via lipolysis in white adipose tissue (WAT) helps improve obesity and metabolic disorders in rodents and humans [5–7]. Moreover, obese subjects have greater quantities of stored TAG and also show a lower lipid turnover rate than non-obese subjects [8].

AMP-activated protein kinase (AMPK), a major energy sensor in the cell, is activated when energy demands increase [9]. Activated AMPK inhibits anabolic pathways and enhances catabolic pathways [9]. Although these roles of AMPK are mostly known in muscle and liver tissue, there have also been several studies proposing that activated AMPK influences obesity and insulin resistance via enhancement of β-oxidation and inhibition of lipogenesis in WAT [5,10]. Previous studies have suggested that some natural compounds are beneficial in the treatment of obesity and metabolic disorders by increasing AMPK activity [10–12].

Adipose tissue in obese patients contains a greater number of macrophages [13]. The paracrine interactions between adipocytes and these recruited macrophages further influence obesity-related inflammation. Such chronic low-grade inflammation in WAT is considered a contributing factor to insulin resistance [14, 15]. Previous studies have reported that several adipokines are abnormally secreted in obese subjects. While adiponectin is significantly decreased [16], pro-inflammatory cytokines including tumor necrosis factor-α (TNF-α) and chemokines such as monocyte chemoattractant protein (MCP)-1 are increased in the obese state [17, 18]. MCP-1 and/or FFA released from adipocytes attract monocytes/macrophages, which subsequently secrete pro-inflammatory cytokines [18]. Adipose tissue macrophages can be categorized as M1 or M2 macrophages according to their distinguishing surface markers [15, 18]. M1 macrophages are characterized by $F4/80^{+}$ $CD11c^{+}$ $CD206^{-}$, whereas M2 macrophages typically express $F4/80^{+}$ $CD11c^{-}$ $CD206^{+}$. M1 or pro-inflammatory macrophages are more dominant than M2 or anti-inflammatory macrophages in the condition of obesity, thereby accelerating adipose tissue inflammation (ATI) [15,18].

Ginger, *Zingiber officinale* Roscoe, has been reported to prevent obesity and its complications [12,19]. 6-gingerol (6G), one of the main bioactive components of ginger, has been extensively studied to elucidate the mechanisms involved in the anti-obesity effect of ginger [20, 21]. Our previous study demonstrated that 6-shogaol (6S), but not 6G, has an inhibitory effect on adipogenesis and lipid accumulation in 3T3-L1 cells [22]. Although Dugasani [23] and Byun et al., [24] compared the anti-inflammatory and anti-cancer activities, respectively, of various ginger components, there is no literature about their effects

on obesity. Thus, we sought to examine which component of ginger may have the greatest anti-adipogenic and anti-lipogenic effects in vitro, and whether GA, a polyphenol present in ginger, can elicits anti-obesity and anti-inflammatory in vivo.

2 Materials and methods

2.1 Chemicals and regents

6G, 8G, 10G, and 6S were purchased from Sigma Chemical (St. Louis, MO). GA was synthesized from curcumin according to a previously reported procedure with some modified methods [25]. Bovine calf serum (BCS), fetal bovine serum (FBS) and antibiotic-antimycotic were obtained from Life Technologies (Grand Island, NY). 3-isobutyl-methylxanthine (IBMX), dexamethasone (DEX), insulin, and Oil red O powder were purchased from Sigma Chemical. Antibodies against sterol regulatory element–binding protein-1 (SREBP-1), carnitine palmitoyltransferase-1 (CPT-1), and peroxisome proliferator-activated receptor-γ (PPARγ) were purchased from Santa Cruz Biotechnology (Santa Cruz, CA). Antibodies against CCAAT/enhancer-binding proteinα (C/EBPα), adipose triglyceride lipase (ATGL), phospho-hormone-sensitive lipase (p-HSL) (Ser565), HSL, fatty acid synthase (FAS), p-AMPKα (Thr172), AMPKα, p-acetyl-CoA carboxylase (p-ACC) (Ser79), and ACC were obtained from Cell Signaling Biotechnology (Beverly, MA). Antibody against peroxisome proliferator-activated receptor gamma coactivator 1α (PGC-1α) was obtained from Abcam (Cambridge, MA). Antibodies against β-actin and glyceraldehyde-3-phosphate dehydrogenase (GAPDH) were purchased from Sigma Chemical.

2.2 Cell culture

3T3-L1 preadipocytes and Raw 264.7 macrophages were obtained from the American Type Culture Collection (Manassas, VA). 3T3-L1 cells were maintained in DMEM (Welgene, Daegu, Korea) containing 10% BCS and 1% antibiotic-antimycotic, and Raw 264.7 cells were cultured in DMEM supplemented with 10% FBS. The cells were incubated in a humidified atmosphere of 5% CO_2 at 37°C.

2.3 Adipogenesis

3T3-L1 cells were seeded at 2.6×10^4 cells per cm^2, and incubated in DMEM containing 10% BCS. The medium was replaced every 2–3 days until the cells reached 100% confluence. After 2 days post-confluence (day 0), the media were exchanged with DMEM supplemented with 10% FBS and an adipogenic cocktail including 0.5 mM IBMX, 1 μM DEX and 5 μg/mL insulin (MDI) for 2 days. On day 2, the medium was then replaced with DMEM supplemented with 10% FBS and 5 μg/mL insulin, and the cells were cultured for a further 2 days. From Day 4, the cells were cultured in 10% FBS-DMEM for 2 additional days.

2.4 Cell viability

To determine the number of viable cells, MTS/PMS mixture (Promega Corp., Madison, WI) was treated for 1 h at 37°C in a humidified 5% CO_2 atmosphere. Converted formazan was detected at 490 nm using a microplate reader (Molecular Devices, Menlo Park, CA).

2.5 Oil red O staining

MDI-induced differentiated 3T3-L1 cells were fixed with 3.7% (v/v) paraformaldehyde and then intracellular lipid droplets were stained with Oil red O solution. For the quantification of the lipid content, the stained Oil red O was extracted with 2-propanol, and the absorbance was measured at 515 nm with a microplate reader.

2.6 Immunoblotting

Cells and tissues were lysed with RIPA buffer (Cell Signaling Biotechnology) and centrifuged (24 100 × *g*, 4°C, 10 min) to collect supernatants separately to the layer of fat. The protein extracts were loaded onto SDS-PAGE and transferred to PVDF membranes (Millipore, Marlborough, MA). The membranes were blocked with 5% skim milk and incubated with specific primary antibodies followed by incubation with HRP-conjugated secondary antibodies. Protein bands were visualized using a chemiluminescence detection kit (Amersham Pharmacia Biotech, Piscataway, NJ).

2.7 Experimental animals and diets

All experiments were approved by the Institutional Animal Care and Use Committee (IACUC) of Seoul National University (SNU-111018-4). Six-week-old male C57BL/6J mice were purchased from Japan SLC Inc. (Hamamatsu, Shizuoka, Japan) and acclimated for 1 week before the study, with free access to chow and water. A total of 47 mice were randomly assigned to the following four groups: standard diet (SD) (10 kcal% fat; $n = 12$), high-fat diet (HFD) (60 kcal% fat; $n = 12$), HFD plus 50 mg/kg body weight GA (HFD-GA50; $n = 12$), or HFD plus 10 mg/kg body weight GA (HFD-GA10; $n = 11$). The diets were purchased from Research Diets, Inc. (New Brunswick, NJ) and provided in the form of pellets for 15 weeks. GA was dissolved in polyethylene glycol (PEG) 200 and introduced to the mice in the HFD-GA groups by oral gavage every day, and mice in the SD and HFD groups were gavaged with vehicle only. After 15 weeks of treatment, mice were sacrificed after an overnight fast, and all efforts were made to minimize suffering. Blood samples were collected from the heart chambers, and then several tissue samples were promptly removed and weighted. Epididymal WAT (EWAT) was snap-frozen in liquid nitrogen and stored at −80°C for RNA and protein analysis.

2.8 Hematoxylin and eosin staining (H&E) and adipocyte cell size assessment

Paraffin sections of formalin-fixed EWATs were stained with H&E for morphological evaluation. The area of each adipocyte was quantified using Image J software (National Institutes of Health, Bethesda, MD).

2.9 Histological analysis

To determine the effect of dietary GA on macrophage infiltration in EWATs, 3-μm-thick sections of EWAT embedded in paraffin were incubated with mouse anti-CD68 mAb at dilutions of 1/200 (Abcam, Cambridge, MA). The sections were then immunostained with HRP polymer (Thermo Fisher Scientific, Fremont, CA) in accordance with the manufacturer's specifications. Crown-like structures (CLS) and CD68-positive cells were counted using Image J software.

2.10 Biochemical analyses

Blood samples were collected in serum separator tubes (Becton Dickinson, Franklin Lakes, NJ) and centrifuged at 1100 × *g* for 20 min. Serum FFAs were determined using a Wako NEFA C test kit (Wako Chemicals, Osaka, Japan). Serum levels of TAG and total cholesterol (TC) were determined by using enzymatic assay kit (Asan Pharmaceutical Co., Seoul, Korea). Liver lipids were isolated by the Folch methods [26], and the hepatic TG and TC levels were measured using the same commercial kit used for the serum analysis.

2.11 qRT-PCR analysis

Total RNA was extracted from EWATs with an Ambion® RNA isolation kit (Life Technologies, Gaithersburg, MD). cDNA was synthesized with a PrimeScript™ 1st strand cDNA Synthesis Kit (Takara, Kyoto, Japan) and qRT-PCR reaction was conducted using specific primers and SYBR Green Master Mix (BioRad, Hercules, CA) with a Bio-Rad CFX96 real-time PCR detection system (BioRad, Hercules, CA). The primers for each transcript are shown in Supporting Information Table 1.

2.12 Trans-well migration assay

RAW264.7 macrophages were plated onto filters in 6.5 mm trans-well inserts in 24-well plates at 2.5×10^4 cells/filter and treated with GA (10 μM). The lower chamber of the well was filled with DMEM in the presence or absence of 3T3-L1 adipocyte conditioned medium (adipocyte-CM) and 0.1% BSA. Cells were then incubated for 2 h. Cells that had migrated into the Type IV collagen-coated membrane were stained with H&E and counted using Image J software.

2.13 Co-culture of adipocytes and macrophages

Adipocytes and macrophages were co-cultured in a contact system. RAW 264.7 macrophages (5×10^4 cells/mL) were plated with differentiated 3T3-L1 adipocytes, and the co-cultures were incubated in serum-free DMEM for 2 h. As a control, adipocytes and macrophages, the numbers of which were equal to those in the co-culture system, were cultured separately and mixed after harvest. GA was added to the co-cultures at 10 μM.

2.14 Statistical analysis

While in vitro results are presented as means ± SD, in vivo data are expressed as means ± SEM. Differences between the negative and positive controls were assessed with unpaired Student's *t*-test. To compare the differences between the differentiated or HFD-fed groups, one-way analysis of variance (ANOVA) with *post hoc* Duncan's test or two-way ANOVA followed by a Bonferroni *post hoc* test was used. A probability value of $p < 0.05$ was used as the criterion for statistical significance.

3 Results

3.1 GA exerts the most potent inhibitory effects on MDI-induced adipogenesis and lipid accumulation in 3T3-L1 cells among treated ginger components

We first compared the effect of gingerols (6G, 8G, and 10G), 6S, or GA, on adipogenesis in 3T3-L1 preadipocytes (Fig. 1A). 6S was used as a positive control according to a previous report [22]. Post-confluent 3T3-L1 preadipocytes were stimulated with MDI to promote differentiation into mature adipocytes in the presence or absence of each ginger compound (40 μM) for 6 days. Photographic and quantitative assessments of intracellular lipid content by Oil red O staining revealed that GA had the most potent anti-adipogenic effect of the tested ginger compounds at the same concentration without affecting cell viability (Fig. 1B–F). Compared to undifferentiated cells, the relative lipid levels of MDI-treated differentiated cells were significantly increased by 3.4-fold. MDI-induced lipid accumulation was most effectively reduced by GA at 40 μM, up to 72.7% (Fig. 1C).

Next, we evaluated the effect of the ginger compounds on adipocyte hypertrophy. Matured 3T3-L1 cells were incubated for 4 days supplemented with the ginger compounds (40 μM). Consistent with its anti-adipogenic effect, GA showed the most potent inhibitory effect on lipid accumulation in mature adipocytes by 18.6%. (Fig. 1E). Collectively, these results suggest that non-toxic concentrations of GA elicits the most potent anti-adipogenic and anti-lipogenic effects in vitro among the five major non-volatile compounds present in ginger.

3.2 GA suppresses adipocyte differentiation and lipid accumulation in 3T3-L1 cells by regulating expression and phosphorylation levels of adipogenic and fatty acid metabolism related proteins

We next tested different concentrations of GA (10, 20, and 40 μM) for 6 days on the adipogenesis of 3T3-L1 cells. Visualized and quantitative data demonstrated that treatment with non-toxic concentrations of GA reduced lipid accumulation in a dose-dependent fashion (Fig. 2A–C). Consistent with these results, protein expression levels of adipogenic transcription factors such as PPARγ and C/EBPα, and lipogenic protein FAS in cells treated with GA at concentrations of 20 and 40 μM were lower than those in MDI only differentiated cells (Fig. 2D). Taken together, we conclude that GA has an anti-adipogenic effect by reducing the expression levels of adipogenic and lipogenic proteins.

Furthermore, we also found that the inhibitory effect of GA on intracellular lipid accumulation in mature 3T3-L1 adipocytes was dose-dependent without affecting cell viability (Fig. 2E–G). To examine how GA inhibits adipocyte hypertrophy, we then investigated whether GA affects fatty acid metabolism related markers. The protein expression levels of SREBP-1 and FAS (lipogenesis markers) were decreased, and the protein expression of PGC-1α and CPT-1 (fatty acid oxidation markers) were increased after treatment with GA at concentrations of 20 and 40 μM (Fig. 2H). We also examined the level of AMPK phosphorylation, as AMPK is a major regulator of cellular anabolic and catabolic pathways. The phosphorylation level of AMPK was increased by GA at 40 μM. These results suggest that GA suppresses adipocyte lipid accumulation via regulation of fatty acid metabolism through AMPK activation.

3.3 GA attenuates weight gain and reduces adipocyte size in HFD-fed mice

To investigate the anti-obesity effect of GA in vivo, we administered GA orally (10, 50 mg/kg) in C57BL/6J mice fed on HFD for 15 weeks. The group receiving 50 mg/kg GA (HFD-GA50) had lower body weights (30.82 ± 0.50 g) than the HFD group (33.87 ± 0.88 g) at 15 weeks ($p < 0.001$; Fig. 3A). Treatment with the lower dose of GA (HFD-GA10) did not have a significant effect on body weight (34.91 ± 0.68 g) over 15 weeks (Fig. 3A). Notably, the final body weight gain of the HFD-GA50 mice was significantly different from control mice fed HFD despite similar caloric intake (Fig. 3B and C). Collectively, these results suggest that GA 50 mg/kg supplementation attenuates DIO without significantly affecting on caloric intake.

Increased fat mass is a major attribute of DIO. We sought to determine whether the decrease in body weight gain was associated with a decrease in fat mass. Consistent with the photographic results (Fig. 3D), visceral fat mass (sum of epididymal, mesenteric, retroperitoneal, and perirenal fat) was significantly lower in the HFD-GA50 versus HFD group (Fig. 3E). In order to determine whether the reductions in fat mass were correlated with adipocyte size, we performed histological analyses of fixed EWAT and quantified adipocyte sizes. As expected, adipocytes from HFD-fed mice were significantly larger than SD-fed mice by up to 2-fold. Interestingly, adipocytes from HFD-GA50 were significantly smaller than adipocytes from the HFD group by 46% (Fig. 3F and G). Analyses of adipocyte size distribution in EWAT revealed that HFD feeding resulted in a significant shift toward larger adipocytes, whereas treatment of HFD-fed mice with GA 50 mg/kg prevented this and restored a normal distribution profile for adipocyte size (Fig. 3H). Taken together, these results suggest that GA supplementation decreases HFD-induced fat mass gain by reducing adipocyte size.

3.4 GA reduces circulating free fatty acid levels

We next evaluated serum and liver lipid concentrations because a decrease in adipose tissue mass can trigger lipodystrophy, an abnormal state of adipose tissue (Table 1). Lipodystrophy can lead to ectopic lipid deposition, caused by an increase in circulating FFAs [27]. Although fasting FFA levels in the HFD group were not significantly different from the SD group, the HFD-GA50 group had significantly lower FFA levels as compared to the HFD group. In contrast, serum TAG and TC levels were not significantly different between treated and non-treated HFD-fed groups. While liver weight and hepatic TC levels were unchanged, hepatic TAG contents in the HFD-GA50 group tended to be lower than in the HFD group ($p = 0.07$). Taken together, our results suggest that GA supplementation is unlikely to induce lipodystrophy.

3.5 GA regulates fatty acid metabolism and mitochondrial biogenesis via activation of AMPK in adipose tissue

To further investigate the mechanisms involved in GA-induced fat mass reduction, we evaluated fatty acid metabolism in EWAT. Since GA decreased circulating FFA levels (Table 1), we first analyzed lipolysis-related biomarkers in EWAT. We determined whether the expression of ATGL, HSL proteins, and the p-HSL at S565 is affected by GA treatment. ATGL expression in HFD-fed mice was 40% lower than in SD-fed mice, whereas the HFD-

GA50 group showed significantly higher ATGL expression than the HFD-fed mice (Fig. 4A). HSL expression in HFD-fed mice was significantly higher than SD-fed mice by up to 2-fold, and this increase was significantly inhibited by GA50 (Fig. 4A). In contrast, p-HSL (Ser565) levels tended to be lower in the HFD group than for SD ($p < 0.07$), and the phosphorylated HSL levels after high fat feeding were significantly increased by treatment with GA 50 mg/kg (Fig. 4A). These results suggest that GA inhibits lipolysis by inhibiting HSL activity in EWAT. We next investigated whether the expression of SREBP-1 and FAS is regulated by GA treatment to examine the effect of GA on lipogenesis in EWAT. As shown in Fig. 4B, GA significantly reduced the expression of SREBP-1 and FAS.

ATGL-medicated TAG degradation can promote β-oxidation by providing a source such as FFA [28]. We next examined the expression of β-oxidation-related genes because GA treatment increased the expression levels of ATGL (Fig. 4A). GA significantly increased *PPARGC1A* (PGC-1α gene), *PPARA* (PPARα gene), and *CPT2* gene expression (Fig. 4C). We also observed that GA significantly enhanced mitochondrial biogenesis-related genes such as nuclear respiratory factor 1 (*NRF1*) and mitochondrial transcription factor A (*TFAM*) in EWAT (Fig. 4C). To further investigate the mechanisms, we assessed AMPK activity in EWAT. P-AMPKα (T172) and p-ACC (S79) expression levels down-regulated by HFD were significantly recovered by treatment with GA 50 mg/kg (Fig. 4D). These results indicate that GA regulates fatty acid oxidation and mitochondrial biogenesis by activating AMPK in EWAT.

3.6 GA suppresses macrophage recruitment and modulates cytokine expression in vitro

We next examined the effect of GA on Raw 264.7 macrophage infiltration into adipocyte-CM using a trans-well system. As shown in Fig. 5A and B, the adipocyte-CM significantly induced macrophage migration, and GA treatment strongly inhibited this migration. This indicates that treatment with GA has an inhibitory effect on adipocyte-CM-induced macrophage chemotaxis.

To further investigate the mechanisms underlying the observed GA-inhibited macrophage migration, we measured gene expression of chemokine C-C Motif Chemokine Lig- and 2 (*CCL2*, MCP-1 gene) and the pro-inflammatory marker *TNF* using a co-culture contact system. Co-cultures of differentiated 3T3-L1 adipocytes and Raw264.7 macrophages in the contact system up-regulated the expression of *CCL2* and *TNF* in comparison to the control group ($p < 0.05$), while addition of GA significantly inhibited this increased expression (Fig. 5C and D).

3.7 GA administration inhibits HFD-induced macrophage infiltration into adipose tissue and reduces ATI by regulating adipokines

We next examined the effect of GA on macrophage infiltration into EWAT and ATI in vivo. Histological examination revealed that the number of CLS in EWAT samples in the HFD group were higher than those in the SD group, which were reduced after GA supplementation (Fig. 6A and B). Moreover, GA suppressed HFD-induced increases in both $CD68^+$ cell recruitment and CD68 gene expression (Fig. 6C and D). We then examined the expression of integrin subunit alpha X (*ITGAX*, M1 marker) and mannose receptor, C type 1

(*MRC1*, M2 marker) in EWAT. HFD significantly increased gene expression of *ITGAX* in adipose tissue, whereas GA treatment significantly reduced this HFD-induced *ITGAX* mRNA expression (Fig. 6E). Unlike *ITGAX*, expression of *MRC1* was not changed significantly by HFD feeding however, GA significantly increased the expression levels in EWAT (Fig. 6F). Taken together, these results indicate that GA suppresses monocyte/macrophage infiltration and promotes an M2 phenotype in EWAT macrophages.

Next, we investigated cytokine gene expression levels involved in macrophage recruitment and ATI. GA prevented the upregulation of mRNA expression of *CCL2* and *TNF* in response to HFD at a concentration of 50 mg/kg in EWAT (Fig. 6G and H). We then analyzed the expression of *ACRP30* (adiponectin gene), an adipokine with anti-inflammatory and insulin-sensitizing effects in obese mice. At a concentration of 50 mg/kg, GA increased the expression level of *ACRP30* (Fig. 6I). These results suggest that GA may be preventing local inflammation in EWAT by inhibiting macrophage recruitment and regulating inflammatory cytokine expression.

4 Discussion

Adipocyte hyperplasia and hypertrophy result in adipose tissue expansion [2]. 3T3-L1 preadipocyte is a useful model to examine adipogenesis and lipid accumulation for understanding these processes [29]. Previous in vitro studies of ginger extracts and its compounds, 6G and 6S, were conducted using 3T3-L1 cells [21, 22]. In the present study, we first compared the effects of ginger compounds on adipocyte differentiation and lipid accumulation using the previously described in vitro model. Our findings show that GA elicits the greater inhibitory effects among tested ginger compounds at 40 μM. To broaden the scope of these studies, we also examined the in vivo effect of GA on obesity using a DIO mouse model, and found that GA has a clear and reproducible anti-obesity effect mainly by limiting fat mass increase in response to high fat feeding.

Although gingerols are highly contained in fresh ginger, those concentrations decrease after processing (e.g. heating or drying) in contrast to shogaols, which increase [30]. In addition, recent finding demonstrate that GA concentrations increase in heated ginger, and exerted anti-cancer effects [24]. Given the different bioactive compounds in fresh vs. processed ginger, we hypothesized that fresh ginger enriched in gingerols may have potent effects in the prevention of obesity and its complications, and that GA as well as 6S may be responsible for the anti-obesity effect of processed ginger.

Energy expenditure in adipose tissue has not received widespread attention over the past few decades because its resting metabolic rate is relatively lower than other metabolic organs such as the liver and muscle [5]. However, recent studies have suggested that the induction of energy expenditure via fatty acid oxidation in WAT is a promising strategy to combat obesity [31–33]. In addition, activating AMPK is also a potential strategy to treat obesity and metabolic disorders by inhibiting anabolic pathways and enhancing catabolic pathways. This is demonstrated by the use of metformin, a type 2 diabetes drug that activates AMPK in liver and muscle [34]. Li et al., reported that 6G improves glucose metabolism by increasing AMPK activity in L6 cells and in vivo rat model [12]. Our findings show that GA also

targets AMPK in both 3T3-L1 adipocytes and EWAT, and further studies are needed to determine how GA specifically activates AMPK in adipocytes. Collectively, these results suggest that GA suppresses body weight gain induced by HFD feeding via the regulation of fatty acid metabolism and mitochondrial biogenesis by activating AMPK in EWAT.

Chronic low-grade inflammation induced by obesity is strongly associated with insulin resistance [15]. Previous studies have identified macrophage infiltration in adipose tissue, suggesting an important link with inflammatory responses [13–15]. Nguyen et al. reported that macrophages infiltrate into hypertrophic adipose tissue and secrete cytokines [35]. Therefore, substances that exert anti-hypertrophic effect may potentially be useful as anti-inflammatory agents. We observed that GA suppresses adipocyte hypertrophy in vitro and in vivo, suggesting the possibility that GA may be used to alleviate inflammation caused by adipose tissues and macrophages. A previous study has shown that macrophages surround the dead and dying adipocytes to form CLS in obese adipose tissue [15]. The number of CLS is indicative of not only the number of dead adipocytes, but also the extent of macrophage recruitment. We observed that GA suppressed the formation of these CLS and the expression levels of CD68 (macrophage marker) in EWAT, suggesting the possibility that GA exerts a protective effect against ATI. Using a trans-well migration assay with a co-culture contact system, we showed GA dramatically inhibits macrophage infiltration and significantly reduced the expression of the pro-inflammatory cytokine *TNF*. These results strongly suggest that GA inhibits ATI via reduction of fat mass and inhibition of macrophage recruitment.

In conclusion, we observed that GA suppressed development of obesity and ATI by reducing adipocyte hypertrophy and inhibiting macrophage infiltration. Taken together, these data support the use of GA in the prevention of obesity and its complications. We propose that further studies are necessary to evaluate the anti-obesity effect of GA in clinical trials.

Supplementary Material

Refer to Web version on PubMed Central for supplementary material.

Acknowledgments

S.S., J.K.K., J.H.Y.P., and K.W.L. conceived and designed the experiments. S.S. and E.L. carried out all in vivo studies. S.S., G.T.K., W.J.J., H.Y., N.R.T., M.Y.C., and S.Y. performed the in vitro studies. S.S. has written the manuscript, and J.H.K, J.Y.K, and J.H.Y.P. proofread this manuscript. J.H.Y.P. and K.W.L. supervised the study.

This work was supported by the Mid-career Researcher Program (2015R1A2A1A10053567) funded by the Ministry of Science, ICT & Future Planning, Republic of Korea. This research was also supported by the Agri-Bio Industry Technology Development Program (514004) and the Agriculture, Food and Rural Affairs Research Center Support Program (710002-07-7sb310), both funded by the Ministry of Agriculture, Food and Rural Affairs, Republic of Korea.

Abbreviations

AMPK	AMP-activated protein kinase
ATGL	adipose triglyceride lipase

ATI	adipose tissue inflammation
CLS	crown-like structures
CM	conditioned medium
CPT-1	carnitine palmitoyltransferase-1
DIO	diet-induced obesity
EWAT	epididymal white adipose tissue
FAS	fatty acid synthase
FFA	free fatty acid
GA	gingerenone A
HSL	hormone-sensitive lipase
PGC-1α	peroxisome proliferator-activated receptor gamma coactivator 1α
SREBP-1	sterol regulatory element–binding protein-1
TAG	triacylglycerol
TC	total cholesterol
TNF-α	tumor necrosis factor-α
6G	6-gingerol
8G	8-gingerol
10G	10-gingerol
6S	6-shogaol

References

1. Després JP, Lemieux I. Abdominal obesity and metabolic syndrome. Nature. 2006; 444:881–887. [PubMed: 17167477]
2. Jo J, Gavrilova O, Pack S, Jou W, et al. Hypertrophy and/or hyperplasia: dynamics of adipose tissue growth. PLoS Comput Biol. 2009; 5:e1000324. [PubMed: 19325873]
3. Ducharme NA, Bickel PE. Lipid droplets in lipogenesis and lipolysis. Endocrinology. 2008; 149:942–949. [PubMed: 18202123]
4. Duncan RE, Ahmadian M, Jaworski K, Sarkadi-Nagy E, et al. Regulation of lipolysis in adipocytes. Annu Rev Nutr. 2007; 27:79–101. [PubMed: 17313320]
5. Flachs P, Rossmeisl M, Kuda O, Kopecky J. Stimulation of mitochondrial oxidative capacity in white fat independent of UCP1: a key to lean phenotype. Biochim Biophys Acta. 2013; 1831:986–1003. [PubMed: 23454373]
6. Qi L, Heredia JE, Altarejos JY, Screaton R, et al. TRB3 links the E3 ubiquitin ligase COP1 to lipid metabolism. Science. 2006; 312:1763–1766. [PubMed: 16794074]
7. Rosen ED, Spiegelman BM. Adipocytes as regulators of energy balance and glucose homeostasis. Nature. 2006; 444:847–853. [PubMed: 17167472]

8. Arner P, Bernard S, Salehpour M, Possnert G, et al. Dynamics of human adipose lipid turnover in health and metabolic disease. Nature. 2011; 478:110–113. [PubMed: 21947005]
9. Towler MC, Hardie DG. AMP-activated protein kinase in metabolic control and insulin signaling. Circ Res. 2007; 100:328–341. [PubMed: 17307971]
10. Lee YS, Kim WS, Kim KH, Yoon MJ, et al. Berberine, a natural plant product, activates AMP-activated protein kinase with beneficial metabolic effects in diabetic and insulin-resistant states. Diabetes. 2006; 55:2256–2264. [PubMed: 16873688]
11. Chen S, Li Z, Li W, Shan Z, et al. Resveratrol inhibits cell differentiation in 3T3-L1 adipocytes via activation of AMPK. Can J Physiol Pharmacol. 2011; 89:793–799. [PubMed: 22017765]
12. Li Y, Tran VH, Kota BP, Nammi S, et al. Preventative effect of Zingiber officinale on insulin resistance in a high-fat high-carbohydrate diet-fed rat model and its mechanism of action. Basic Clin Pharmacol Toxicol. 2014; 115:209–215. [PubMed: 24428842]
13. Weisberg SP, McCann D, Desai M, Rosenbaum M, et al. Obesity is associated with macrophage accumulation in adipose tissue. J Clin Invest. 2003; 112:1796–1808. [PubMed: 14679176]
14. Xu H, Barnes GT, Yang Q, Tan G, et al. Chronic inflammation in fat plays a crucial role in the development of obesity-related insulin resistance. J Clin Invest. 2003; 112:1821–1830. [PubMed: 14679177]
15. Osborn O, Olefsky JM. The cellular and signaling networks linking the immune system and metabolism in disease. Nat Med. 2012; 18:363–374. [PubMed: 22395709]
16. Maeda N, Shimomura I, Kishida K, Nishizawa H, et al. Diet-induced insulin resistance in mice lacking adiponectin/ACRP30. Nat Med. 2002; 8:731–737. [PubMed: 12068289]
17. Sartipy P, Loskutoff DJ. Monocyte chemoattractant protein 1 in obesity and insulin resistance. Proc Natl Acad Sci USA. 2003; 100:7265–7270. [PubMed: 12756299]
18. Kammoun HL, Kraakman MJ, Febbraio MA. Adipose tissue inflammation in glucose metabolism. Rev Endocr Metab Disord. 2014; 15:31–44. [PubMed: 24048715]
19. Mahmoud R, Elnour W. Comparative evaluation of the efficacy of ginger and orlistat on obesity management, pancreatic lipase and liver peroxisomal catalase enzyme in male albino rats. Eur Rev Med Pharmacol Sci. 2013; 17:75–83. [PubMed: 23329526]
20. Saravanan G, Ponmurugan P, Deepa MA, Senthilkumar B. Anti-obesity action of gingerol: effect on lipid profile, insulin, leptin, amylase and lipase in male obese rats induced by a high-fat diet. J Sci Food Agric. 2014; 94:2972–2977. [PubMed: 24615565]
21. Tzeng TF, Liu IM. 6-gingerol prevents adipogenesis and the accumulation of cytoplasmic lipid droplets in 3T3-L1 cells. Phytomedicine. 2013; 20:481–487. [PubMed: 23369342]
22. Suk S, Seo SG, Yu JG, Yang H, et al. A Bioactive constituent of ginger, 6-shogaol, prevents adipogenesis and stimulates lipolysis in 3T3-L1 adipocytes. J Food Biochem. 2016; 40:84–90.
23. Dugasani S, Pichika MR, Nadarajah VD, Balijepalli MK, et al. Comparative antioxidant and anti-inflammatory effects of [6]-gingerol, [8]-gingerol, [10]-gingerol and [6]-shogaol. J Ethnopharmacol. 2010; 127:515–520. [PubMed: 19833188]
24. Byun S, Lim S, Mun JY, Kim KH, et al. Identification of a dual inhibitor of janus kinase 2 (JAK2) and p70 ribosomal S6 kinase1 (S6K1) pathways. J Biol Chem. 2015; 290:23553–23562. [PubMed: 26242912]
25. Venkateswarlu S, Ramachandra M, Rambabu M, Subbaraju GV. Synthesis of gingerenone-A and hirsutenone. Indian J Chem B. 2001; 40:495–497.
26. Folch J, Lees M, Sloane-Stanley G. A simple method for the isolation and purification of total lipids from animal tissues. J Biol chem. 1957; 226:497–509. [PubMed: 13428781]
27. Fiorenza CG, Chou SH, Mantzoros CS. Lipodystrophy: pathophysiology and advances in treatment. Nat Rev Endocrinol. 2011; 7:137–150. [PubMed: 21079616]
28. Gaidhu MP, Ceddia RB. The role of adenosine monophosphate kinase in remodeling white adipose tissue metabolism. Exerc Sport Sci Rev. 2011; 39:102–108. [PubMed: 21206283]
29. Poulos SP, Dodson MV, Hausman GJ. Cell line models for differentiation: preadipocytes and adipocytes. Exp Biol Med (Maywood). 2010; 235:1185–1193. [PubMed: 20864461]

30. Ali BH, Blunden G, Tanira MO, Nemmar A. Some phytochemical, pharmacological and toxicological properties of ginger (Zingiber officinale Roscoe): a review of recent research. Food Chem Toxicol. 2008; 46:409–420. [PubMed: 17950516]

31. Jbilo O, Ravinet-Trillou C, Arnone M, Buisson I, et al. The CB1 receptor antagonist rimonabant reverses the diet-induced obesity phenotype through the regulation of lipolysis and energy balance. FASEB J. 2005; 19:1567–1569. [PubMed: 16009704]

32. Boudina S, Graham TE. Mitochondrial function/dysfunction in white adipose tissue. Exp Physiol. 2014; 99:1168–1178. [PubMed: 25128326]

33. Semple RK, Crowley VC, Sewter CP, Laudes M, et al. Expression of the thermogenic nuclear hormone receptor coactivator PGC-1alpha is reduced in the adipose tissue of morbidly obese subjects. Int J Obes Relat Metab Disord. 2004; 28:176–179. [PubMed: 14557831]

34. Zhou G, Myers R, Li Y, Chen Y, et al. Role of AMP-activated protein kinase in mechanism of metformin action. J Clin Invest. 2001; 108:1167–1174. [PubMed: 11602624]

35. Nguyen MT, Favelyukis S, Nguyen AK, Reichart D, et al. A subpopulation of macrophages infiltrates hyper-trophic adipose tissue and is activated by free fatty acids via Toll-like receptors 2 and 4 and JNK-dependent pathways. J Biol Chem. 2007; 282:35279–35292. [PubMed: 17916553]

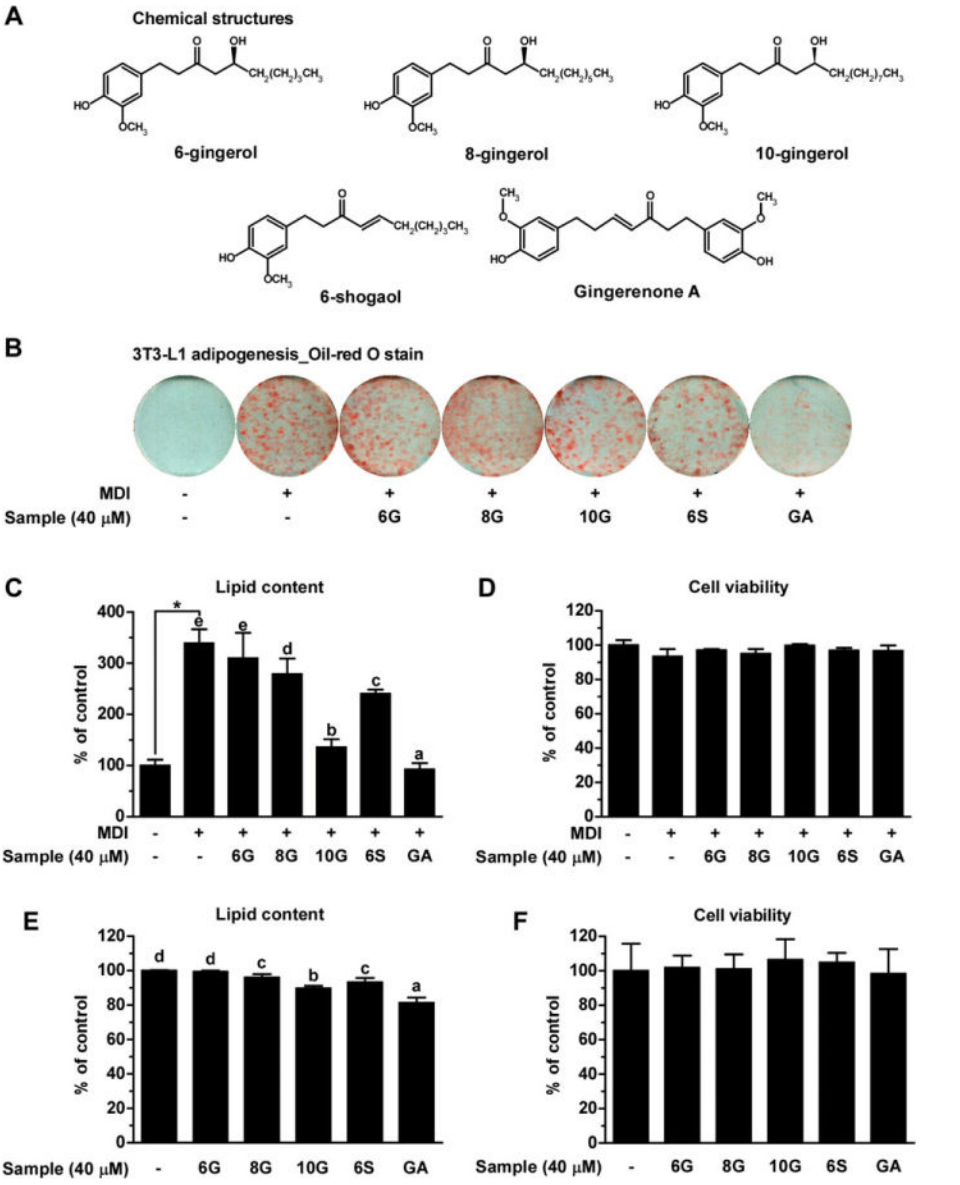

Figure 1.

GA is the most potent anti-adipogenic and anti-lipogenic agent among the five bioactive compounds present in ginger on 3T3-L1 cells. (A) Chemical structure of five bioactive compounds present in ginger. (B) The undifferentiated preadipocytes, MDI-induced adipocytes, and adipocytes differentiated with five bioactive compounds were subjected to Oil red O staining for visualization of lipid droplets. (C) Stained intracellular lipid droplets were extracted with 2-propanol and then quantified by measuring the absorbance at 515 nm. Lipid content for each group was expressed relative to that of undifferentiated cells (designated as 100%). (D) Effect of five ginger compounds on the viability of 3T3-L1preadipocytes during adipogenesis. (E) Quantification of lipid content in matured adipocytes treated with or without ginger components. (F) Effect of ginger components on the viability of matured adipocytes. Data are representative of three independent experiments, which are presented as means ± SD. Statistical significance between the

undifferentiated and differentiated control was determined using Student's *t*-test. One-way ANOVA was used with Duncan's multiple rage tests for *post hoc* analysis. Different letters indicate statistically significant differences at $p < 0.05$.

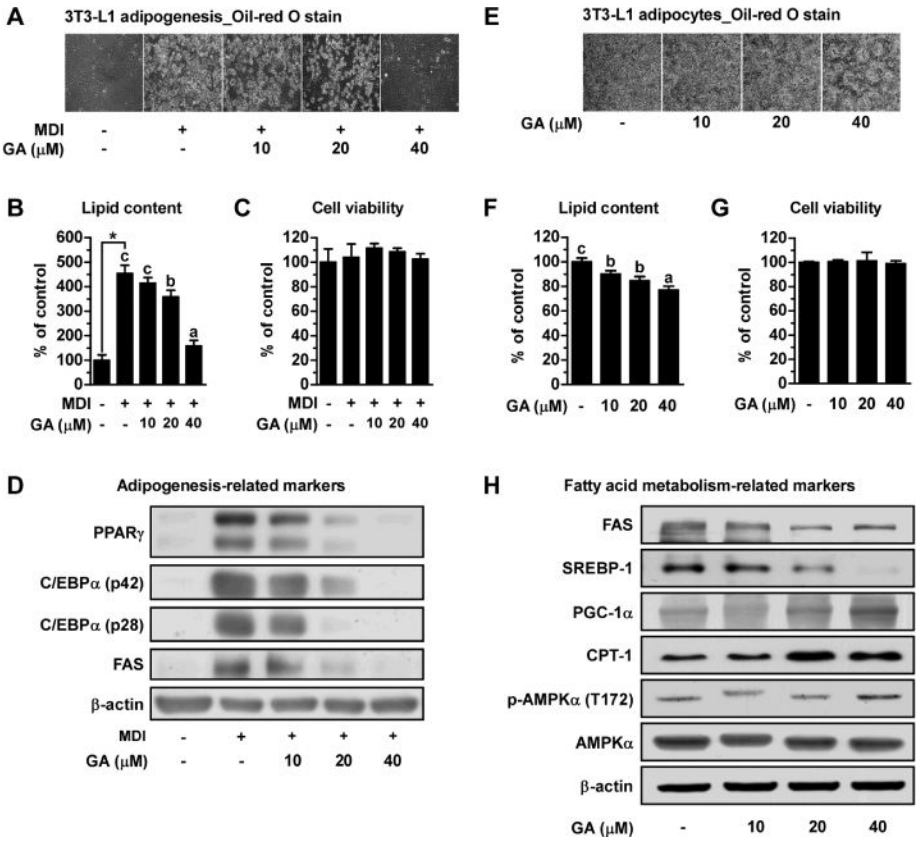

Figure 2.

GA inhibits hyperplasia and hypertrophy of 3T3-L1 cells, and regulates expression or phosphorylation levels of adipogenic and fatty acid metabolism related proteins. (A and B) Visualization and quantification data of intracellular lipid content treated with GA at various concentrations during adipogenesis. (C) Effect of GA on the viability of 3T3-L1 preadipocytes. (D) Protein levels of PPAR-γ, C/EBP-α, and FAS were examined after 6 days of differentiation as determined by Western blot analysis. β-actin was used as loading control. Matured 3T3-L1 cells were incubated for 4 days and supplemented with the GA, and (E) the representative optical images and (F) the relative intracellular lipid content of 3T3-L1 adipocytes were obtained. (G) Effect of GA on the viability of 3T3-L1 adipocytes. (H) Western blot analyses of lipogenesis-related proteins (SERBP-1 and FAS), fatty acid oxidation-related proteins (PGC-1α and CPT-1), p-AMPKα (T172) and total AMPKα.

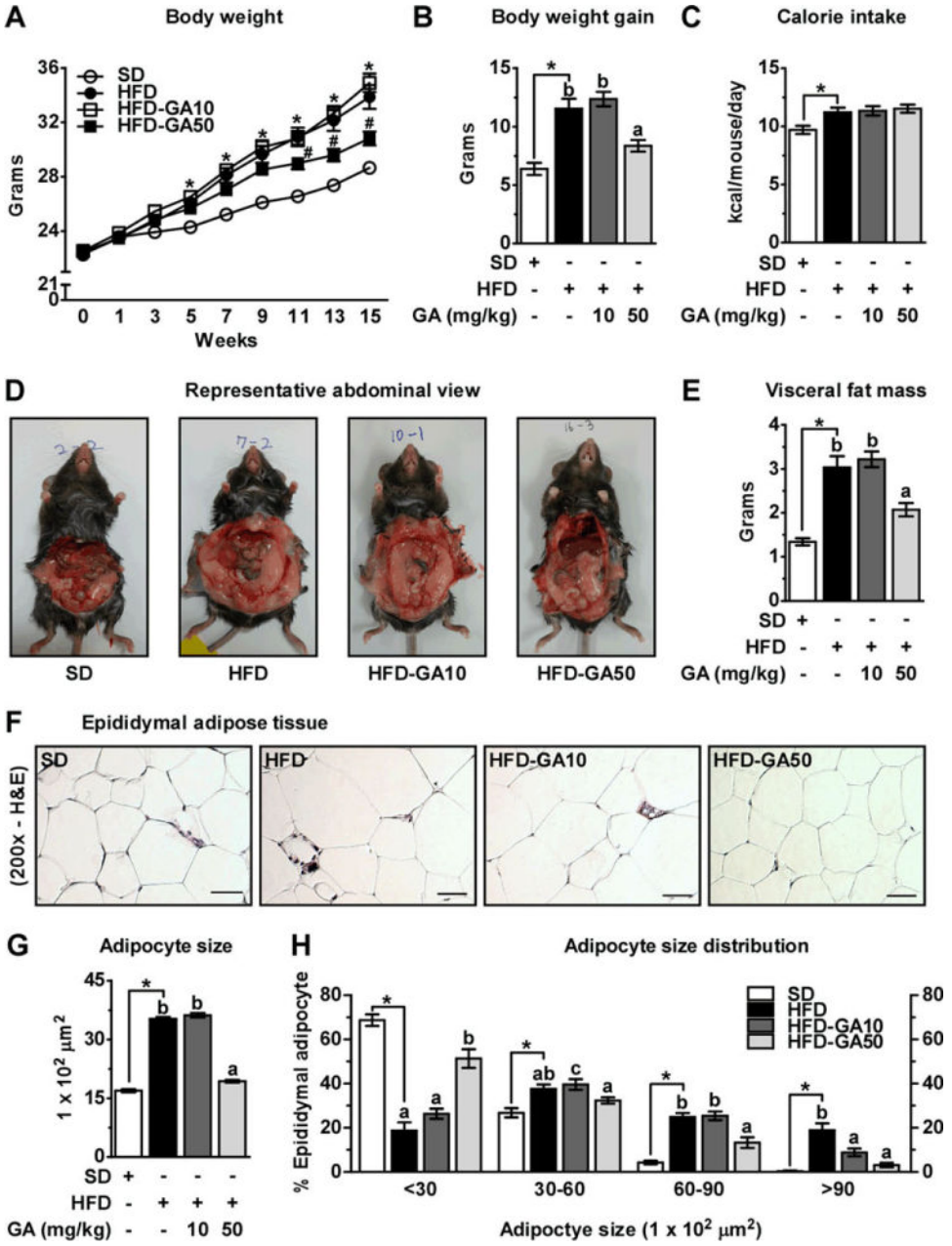

Figure 3.

GA administration suppresses weight gain and reduces adipocyte size in HFD-fed mice. (A) Body weight curves, (B) body weight gain, and (C) energy intake (kcal/mouse/day) over 15 weeks. (D) Representative abdominal view. (E) Weight of visceral fat mass. (F) Sections of EWAT were stained with H&E. Representative images are shown. Scale bar, 200 µm. (G) Adipocyte size area. (H) Adipocyte size distribution of EWAT. The time course values of change in body weight were analyzed by two-way ANOVA followed by a Bonferroni *post hoc* test (*$p < 0.05$ HFD versus SD; $^{\#}p < 0.05$ GA-treatment groups versus HFD). Unpaired Student's *t*-test was used to detect statistically significant differences between SD and HFD

group (*$p < 0.05$). Then, one-way ANOVA was used with Duncan's multiple rage tests for *post hoc* analysis to compare the differences among the three HFD groups.

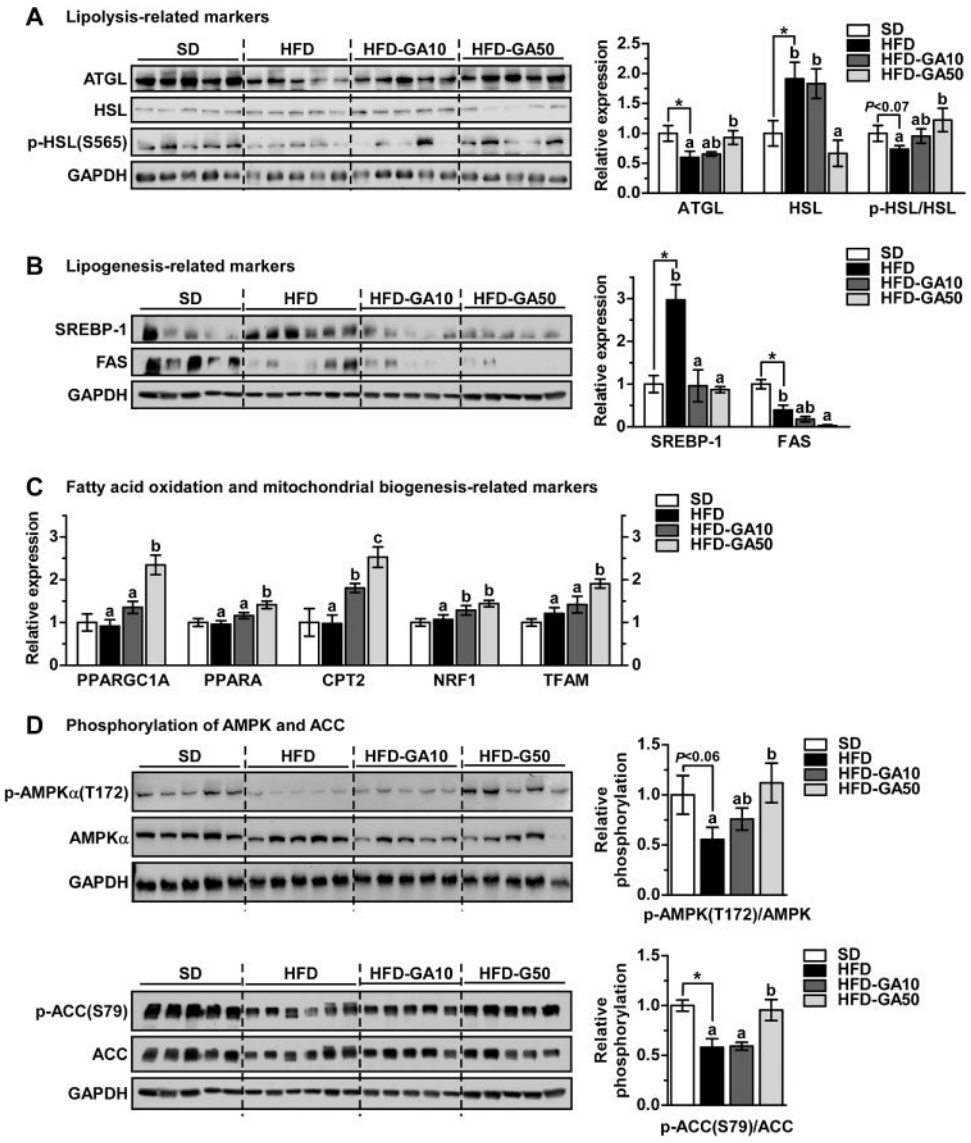

Figure 4.

GA treatment regulates the expression of fatty acid metabolism and mitochondrial biogenesis related markers via activation of AMPK in EWAT. Western blot analysis of (A) lipolysis related proteins (ATGL, HSL, and p-HSL (S565)) in EWAT. Western blot analysis of (B) lipogenesis related proteins (SREBP-1 and FAS) in EWAT. GAPDH was used as a loading control. The expression levels were quantified using Image J software. (C) Total RNA was isolated and qRT-PCR was performed. Fatty acid oxidation related genes (*PPARGC1A*, *PPARA*, and *CPT2*) and mitochondrial biogenesis related genes (*NRF1* and *TFAM*). (D) Western blot analysis of p-AMPKα (T172), total AMPK, p-ACC (S79), and total ACC in EWAT.

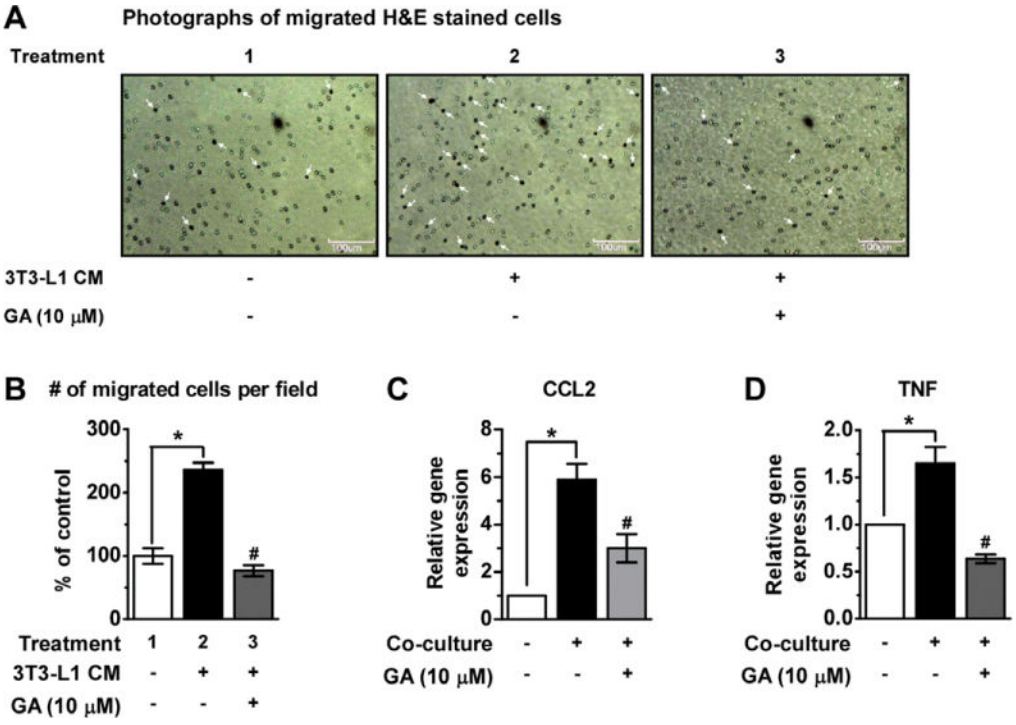

Figure 5.

GA inhibits macrophage recruitment and modulates adipokines expression. RAW264.7 cells were plated in 6-well plate containing differentiated 3T3-L1 cells. As a control, RAW264.7 cells and differentiated 3T3-L1 cells were separately cultured for 2 h. The migration of RAW264.7 cells through a type IV collagen-coated trans-well filter was assessed with 3T3-L1 CM and GA (10 μM). (A) Photographs of migrated H&E stained cells (white arrows) are shown (× 100). (B) Quantitative analysis of the migrated cells. (C, D) total RNA was isolated from RAW264.7 cells and 3T3-L1 cells (control) and RAW264.7/3T3-L1 co-cultures (co-culture), and real-time RT-PCR was performed. Alteration of gene expression of pro-inflammatory cytokines (*CCL2* and *TNF*) by co-culture in the contact system. Values were analyzed using unpaired Student's *t*-test. $^{*}p < 0.05$ control versus co-culture control, $^{\#}p < 0.05$ GA-treated versus co-culture control.

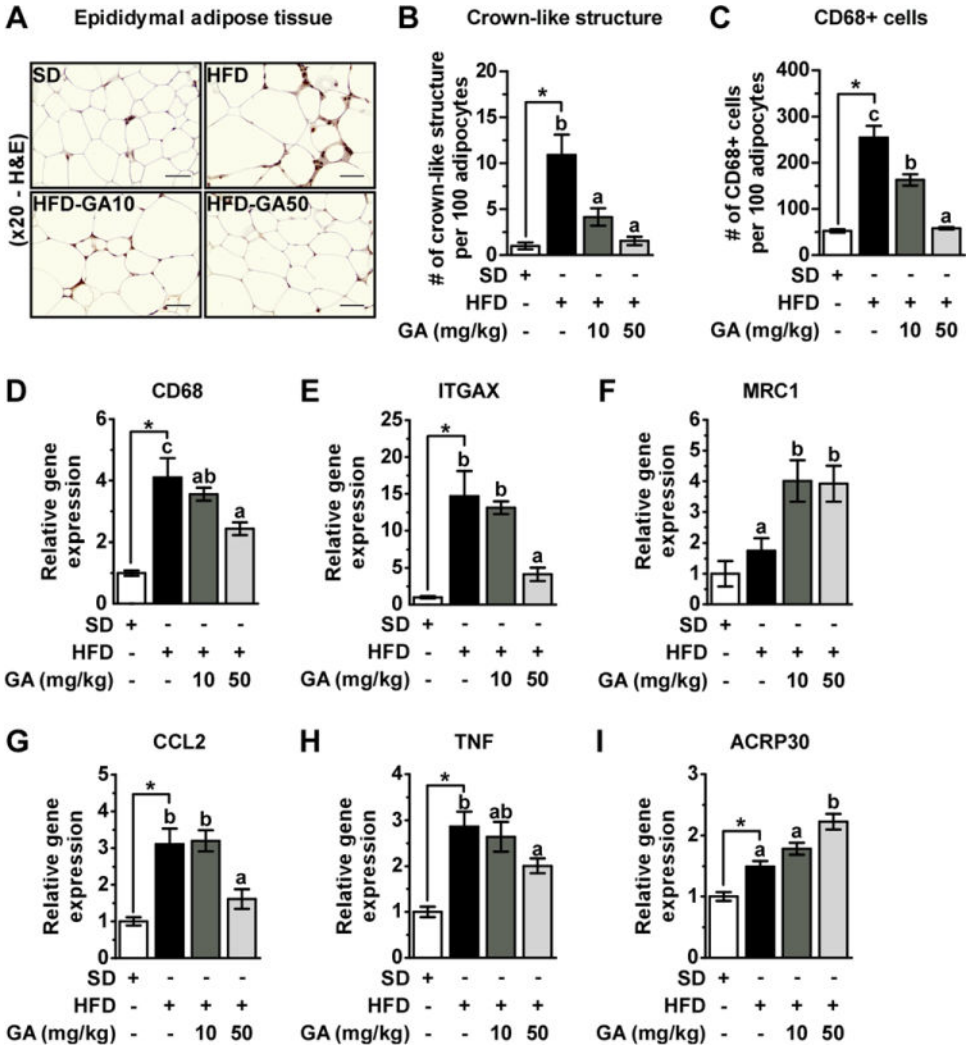

Figure 6.

GA prevents aggravation of macrophage infiltration induced by HFD and regulates inflammation-related cytokines in EWAT. (A) Immunohisto-chemical detection of CD68 in EWAT. Macrophages are stained brown. (200×), (B) number of CLS, and (C) total number of infiltrated monocyte/macrophage into EWAT, which was quantified by counting CD68-positive cells per 100 adipocytes. (D) *CD68*, (E) *ITGAX*, and (F) *MRC1* genes expression in EWAT. (G) *CCL2* (H) *TNF*, and (I) *ACRP30* genes expression in EWAT. All values were normalized to GAPDH.

Table 1

Serum and liver biochemical parameters

	SD	HFD	HFD-GA10	HFD-GA50
Serum FFA (mEq/L)	1.36 ± 0.05	1.36 ± 0.09[a)]	1.47 ± 0.09[a)]	1.11 ± .0.07[b)]
Serum TAG (mg/dL)	71.35 ± 3.40	81.84 ± 6.81	74.68 ± 5.41	70.11 ± 6.92
Serum TC (mg/dL)	112.23 ± 3.80	161.38 ± 4.55*	170.00 ± 5.52	158.44 ± 6.67
Liver weight (g)	1.06 ± 0.02	1.00 ± 0.04	1.04 ± 0.01	1.04 ± 0.02
Liver TAG (mg/g liver)	43.54 ± 3.52	36.69 ± 4.55	36.08 ± 3.15	25.86 ± 3.11 (P = 0.07)
Liver TC (mg/g liver)	7.57 ± 0.81	5.67 ± 0.60	6.59 ± 0.68	5.43 ± 0.87

Data represent mean values ± SEM. Unpaired Student's t-test was used to detect statistically significant differences between SD and HFD group (*$p < 0.05$). Then, one-way ANOVA was used with Duncan's multiple rage tests for *post hoc* analysis to compare the differences among the three HFD groups. Different letters indicate statistically significant differences. Differences were considered significant at $p < 0.05$. FFA, free fatty acid; TAG, triacylglycerol; TC, total cholesterol.